PHOTONICS Research

Sensing and tracking enhanced by quantum squeezing

Chuan Xu,[1] Lidan Zhang,[1] Songtao Huang,[1] Taxue Ma,[1] Fang Liu,[1,2] Hidehiro Yonezawa,[3] Yong Zhang,[1,*] and Min Xiao[1,4,5]

[1]National Laboratory of Solid State Microstructures, College of Engineering and Applied Sciences, and School of Physics, Nanjing University, Nanjing 210093, China
[2]Department of Physics, Nanjing Tech University, Nanjing 211816, China
[3]Centre for Quantum Computation and Communication Technology, School of Engineering and Information Technology, University of New South Wales, Canberra, Australian Capital Territory 2600, Australia
[4]Department of Physics, University of Arkansas, Fayetteville, Arkansas 72701, USA
[5]e-mail: mxiao@uark.edu
*Corresponding author: zhangyong@nju.edu.cn

Received 24 January 2019; revised 25 March 2019; accepted 26 March 2019; posted 27 March 2019 (Doc. ID 357871); published 3 May 2019

Quantum sensing, along with quantum communications and quantum computing, is commonly considered as the most important application of quantum optics. Among the quantum-sensing experiments, schemes based on squeezed states of light are popular choices due to their natural quadrature components. Since the first experimental demonstration of quantum-squeezing-enhanced phase measurement beyond the shot-noise limit in 1987, quantum-squeezing techniques toward practical sensing and tracking have been extensively investigated. In this paper, we briefly review the recent developments of quantum squeezing and its applications in several advanced systems for measurements of position, rotation, dynamic motion, magnetic fields, and gravitational waves. We also introduce the recent experimental efforts to combine the quantum-squeezing lights into fiber sensing systems.

https://doi.org/10.1364/PRJ.7.000A14

1. INTRODUCTION

Over the past 30 years, squeezed states of light have been exploited as an important quantum resource in different fields, such as continuous-variable quantum teleportation [1,2] and quantum computing [3], quantum error correction coding [4,5], quantum state engineering [6–8], quantum imaging [9,10], and precision measurement and sensing [11–17]. Because the noise of certain quadrature components of squeezed light is lower than that of coherent light, squeezed light is capable of surpassing the shot-noise limit (SNL) for the high precision measurement of a physical parameter. Obviously, squeezed light sources are necessary to optimize and upgrade the performance of an optical sensing system. The main methods used to generate squeezed states are the second and third nonlinear processes, e.g., parametric downconversion (PDC) [18] and four-wave mixing (FWM) [19]. Squeezed states of light have been obtained with different experimental systems, such as atomic ensembles [20–22], fibers [23–25], mechanical resonators [26,27], microcavities [28–30], and optical parametric oscillator (OPO) cavities [31–33]. In this review, we focus on the single-mode squeezed light generated in a cavity, as it is a mature method to achieve high-quality squeezed states of light. To date, the highest squeezing factor of 15 dB has been obtained by employing a sub-threshold OPO cavity [33].

Single-mode squeezed light has proven very useful in many practical systems of precision measurement, such as phase estimation [16] and tracking [12], optical magnetometers [11], biological measurement [13], small displacement measurement [34], and gravitational wave (GW) detection [14,35], with the purpose being to improve the signal-to-noise ratio (SNR). For instance, with squeezing, the error of a tracked phase was well below the coherent-state limit [12]. Squeezing was applied in a magnetometer with the sensitivity enhanced by 3.2 dB [11] and biological measurements for which quantum noise was surpassed by 42% [13]. Moreover, quantum-squeezing-enhanced fiber Sagnac [36] and Mach–Zehnder interferometers (MZIs) [37] were demonstrated in 2010 and 2017, respectively. Goda *et al.* improved the displacement sensitivity of a prototype GW detector by 44% with a squeezed vacuum [38]. Subsequently, the GEO 600 was the first GW detector employing squeezing leading to a broadband noise reduction of up to 3.5 dB [35]. Thereafter, noise of the LIGO interferometer was beyond the SNL of 2.15 dB with squeezed-light injection, and the frequency range was extended down to 150 Hz [14].

It should be noted that other quantum light sources can also be utilized in quantum sensing. For example, quantum correlation [39–41] and quantum entanglement created by multimode squeezed states [42–54] have potential applications in

quantum computing [3], quantum networks [53], and squeezing-enhanced imaging [55]. The phase sensitivity of the interferometer can be theoretically improved to the Heisenberg limit of $1/N$ [56–62] by using the NOON state [60] or SU(1,1) interferometry [56,62]; here N is the average photon number for detection. One can see the references for details.

In this paper, we review the recent progress and applications of single-mode squeezed states of light for optical sensing and tracking. In Section 2, we present the basic principle and the primary measurement schemes such as the interferometer, homodyne detection, and heterodyne detection with squeezed-light injection. The applications of these schemes such as phase tracking, position and rotation measurement, magnetic field measurement, GW detection, and fiber sensing are introduced in Section 3. The future prospects for squeezing are presented in Section 4.

2. BASIC PRINCIPLE AND PRIMARY MEASUREMENT SCHEMES WITH SQUEEZING

A. Basic Principle of Squeezed Light

A nearly monochromatic electromagnetic field can be regarded as a function of a pair of non-commuting quadrature components in phase space, which are normally called amplitude quadrature $\hat{X}$ and conjugate phase quadrature $\hat{Y}$. According to Heisenberg's uncertainty principle, non-commuting observables cannot be precisely measured simultaneously, and their uncertainty relation is

$$\Delta^2\hat{X}\Delta^2\hat{Y} \geq 1. \tag{1}$$

For a coherent state, the fluctuations of different quadrature components are identical in phase space and equal to zero-point fluctuations (also called shot noise), i.e., $\Delta^2\hat{X} = \Delta^2\hat{Y} = 1$. Figure 1(a) shows a representation of a coherent state using the phasor diagram. When measuring weak signals such as GWs with a coherent state, the experimental data generally exhibit these fluctuations. To improve the sensitivity of the measurement while obeying Heisenberg's uncertainty principle, squeezed light is introduced in which the fluctuations of one quadrature component are squeezed at the expense of an expansion for the other. In this case, the fluctuations are given by $\Delta^2\hat{X} = e^{-2r} < 1$ and $\Delta^2\hat{Y} = e^{2r} > 1$, where r is called the squeezing factor [63]. During a measurement process, one can use the squeezed quadrature component to enhance the precision. In Fig. 1, we present several typical coherent states and squeezed states.

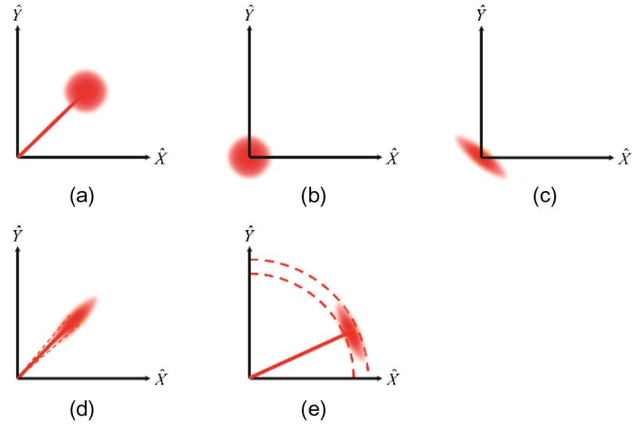

Fig. 1. Representation of different states in the phasor diagram: (a) coherent state, (b) vacuum state, (c) vacuum-squeezed state, (d) phase-squeezed state, and (e) amplitude-squeezed state.

To obtain squeezed light, the main methods employ phase-dependent nonlinear processes, such as FWM and PDC. In 1985, Slusher *et al.* first observed squeezing using FWM [19]; then Wu *et al.* obtained 3-dB squeezed light via a PDC process [18]. Thereafter, researchers have generated squeezed states using versatile methods with significant technical improvements [33,64–67]. Because the performance of a quantum-sensing system strongly depends on the squeezed light, researchers have made great efforts in the improvement of the squeezing factor. To date, the greatest squeezing is 15 dB below the SNL, which is obtained through an optical parametric amplification (OPA) process in a periodically poled $KTiOPO_4$ (PPKTP) crystal [33].

OPA happens in a nonlinear crystal with a second-order susceptibility $\chi^{(2)}$. A pump field and a signal field are injected into the crystal. In the OPA process, the pump field is converted to the signal and idler fields. Because of energy conservation, the sum of the frequencies of the signal and idler fields equals the frequency of the pump field. Similarly, the momentum conservation requires phase matching of the interacting wavevectors. In addition, the temperature of the nonlinear crystal must be carefully controlled for proper phase matching.

Taking the vacuum state as an example, the manner in which the nonlinear process generates squeezed light is depicted in Fig. 2 [68]. Consider a short segment of a $\chi^{(2)}$ nonlinear crystal interacting with a vacuum state $E^{\text{in}}_{\text{vac},f}$ and coherent state E^{in}_{2f}, where E denotes the amplitude of the electric field, and f and $2f$ denote the optical frequencies of the vacuum state and the coherent state, respectively. The red and orange regions in Fig. 2 represent the fluctuations of the vacuum state before and after the OPA process, which describes the squeezing effect. The dielectric polarization $P(E)$ inside the crystal generates

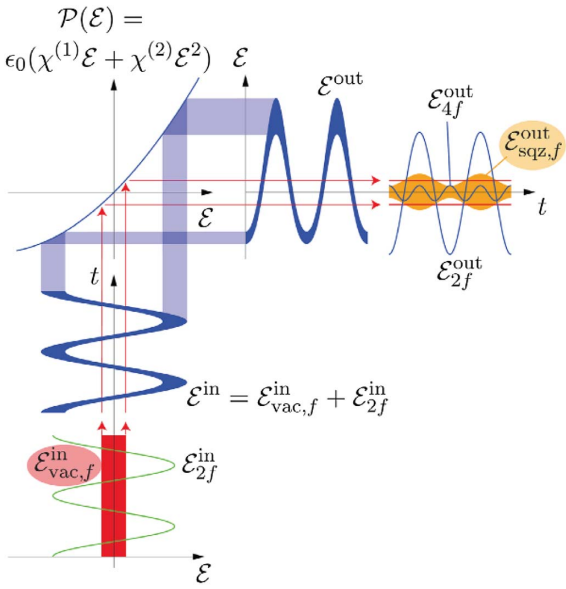

Fig. 2. Schematic of degenerate OPA and graph of dielectric polarization $P(E) = \varepsilon_0(\chi^{(1)}E + \chi^{(2)}E^2)$ representing the second-order nonlinear process in the crystal. Adapted with permission from Ref. [68].

a vacuum-squeezed state via OPA. Because of phase mismatch, the unwanted components such as E_{4f}^{out} are greatly suppressed, which ensures the purity of the squeezed light. The graph of $P(E)$ illustrates the phase dependence of the noise of the vacuum field on the pump field.

The standard method to detect squeezing is balanced homodyne detection (BHD). A strong local oscillator (LO) and a squeezed light with the same optical frequency interfere on a 50/50 beam splitter (BS) and then are coupled to a pair of balanced detectors [Fig. 3(a)]. After isolating the low-frequency signal and reserving the first-order terms, the fluctuation of the BHD output is given by

$$\Delta i_{-} \cong \alpha(\delta\hat{X}\cos\theta + \delta\hat{Y}\sin\theta), \tag{2}$$

where α is the amplitude of the LO, $\delta\hat{X}$ and $\delta\hat{Y}$ are the fluctuations in the amplitude and phase quadrature components, respectively, and θ is the relative phase between the LO and the squeezed light. The output contains the fluctuations of the squeezed light multiplying by the amplitude of the LO. By modifying the relative phase θ, one is able to measure the fluctuations of any quadrature component $\delta\hat{X}^{\theta} = \delta\hat{X}\sin\theta + \delta\hat{Y}\cos\theta$ and then reconstruct the state [69].

B. Primary Measurement Schemes with Squeezing

Most optical precision measurements are based on interferometry, homodyne detection, and heterodyne detection. The optical phase difference of the two arms provides a measure of the signal sought. However, vacuum noise introduced through the unused port limits the measurement precision [70]. Replacing vacuum noise by injecting squeezed light into the unused port can significantly suppress the noise and improve the SNR. Many experiments have demonstrated squeezing-enhanced precision measurement. In this section, we briefly review two typical configurations, i.e., the squeezing-enhanced MZI [71] and the polarization interferometer [72].

An MZI [Fig. 3(b)] takes in an incident monochromatic coherent light beam and a vacuum-squeezed beam, mixes them at BS1(50/50), and splits them into two arms. The two beams are brought together again to interfere at BS2(50/50) and finally are detected by two photodetectors. The frequencies of the two incident light beams are same. The relative phase ϕ of the two arms is kept equal to $\pi/2$ for the optimal SNR. Without injection of a squeezed light, the minimal measurable phase difference is

$$\Delta\phi_{\min} = \frac{1}{\sqrt{N}}, \tag{3}$$

where N is the average photon number of the coherent beam of light. If a vacuum-squeezed component is used in detection, the sensitivity $\Delta\phi$ improves by a factor e^{-r} for a lossless process. In practice, the enhancement is degraded by the system loss. The above analysis is also valid for other types of interferometers, such as the Sagnac interferometer and the Michelson interferometer [73].

The first squeezing-enhanced experiment based on MZI was performed by Xiao *et al.* [71]. The squeezed vacuum was produced from an OPO cavity and injected through the unused port of the MZI. A phase dither was placed in one arm.

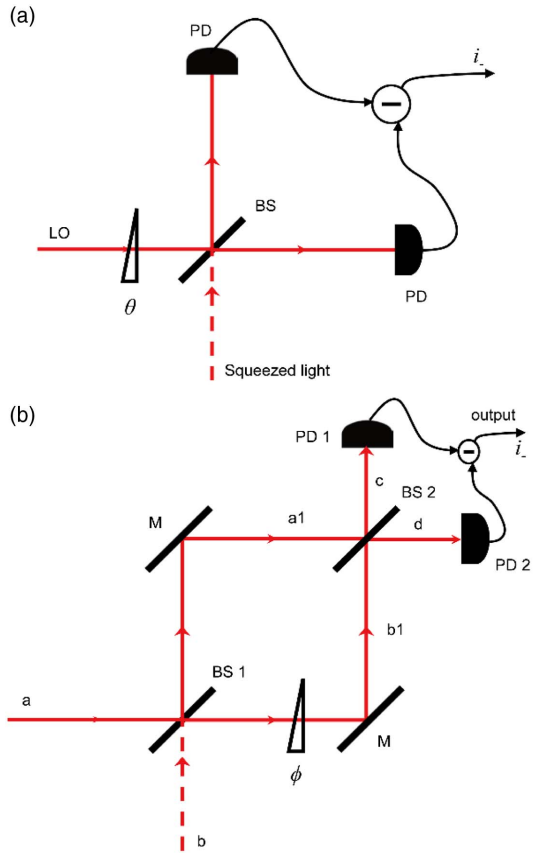

Fig. 3. (a) Schematic of balanced homodyne detection. PD, photodetector. (b) Setup of an MZI. M, mirror. Coherent light illuminates port a of the MZI, while a vacuum state (or squeezed state) is injected via port b.

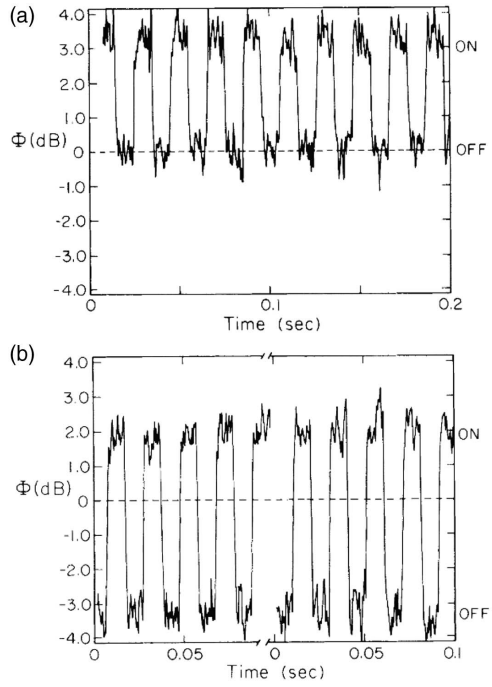

Fig. 4. Square-wave phase signal is obtained with (a) vacuum and (b) squeezed vacuum. Adapted with permission from Ref. [71].

As shown in Fig. 4, a 3-dB improvement of the SNR was observed using squeezed light.

A squeezing-enhanced polarization interferometer [Fig. 5(a)] [72] was proved to be very sensitive in the detection of polarizations and magnetic fields [11]. A KTP crystal was placed in a cavity to generate squeezed light, which was subsequently coupled with a coherent light using a polarization beam splitter (P1) and then passed through a polarization rotator (PR). A half-wave plate and the second polarization beam splitter (P2) served as a BS for BHD where the coherent light acted as an LO. When the rotator was removed and the squeezed light was blocked, the fluctuation in the BHD output corresponded to an SNL. The polarization rotation signal was detected by BHD. Traces (a), (b), and (c) in Fig. 5(b) were obtained with squeezed light, the vacuum state, and anti-squeezed light input at the unused port, respectively. With squeezing injection, the SNR was improved by 1.8 dB relative to the vacuum.

Besides, heterodyne detection is capable of measuring the difference in frequency of two fields to avoid low-frequency noise. The technique was applied to Doppler anemometry to obtain the velocity of gas flows and improved the SNR by 1 dB using amplitude-squeezed light [74].

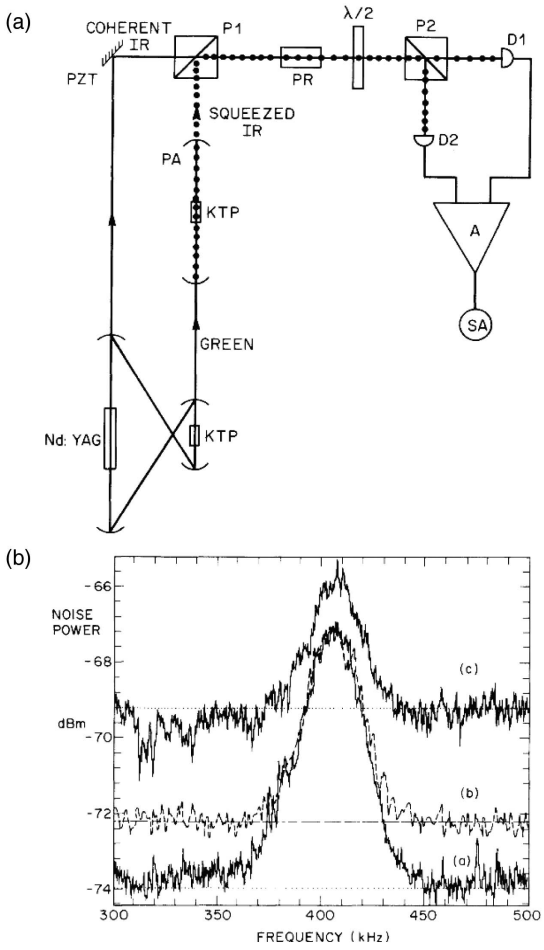

Fig. 5. (a) Polarization interferometer. (b) Polarization rotation signal and noise. Adapted with permission from Ref. [72].

3. SQUEEZING-ENHANCED APPLICATIONS IN VARIOUS FIELDS

A. Position and Rotation Measurement

The measurement of the point spot of a laser beam is used in many areas such as atomic force microscopy [75], ultraweak absorption measurements [76], and single-molecule tracking in biology [13,77]. The position of the spot can be defined as the mean position of all photons in the beam, the measurement precision of which is constrained by quantum fluctuation. The transverse displacement resolution of a TEM_{00} laser beam is given by [78]

$$D_{\mathrm{QNL}} = \frac{w_0}{2\sqrt{N_{\mathrm{tot}}}}, \tag{4}$$

where w_0 is the waist of the beam and N_{tot} is the total photocurrent; QNL is an abbreviation for the quantum noise limit.

Any displacement modulation of the TEM_{00} mode is transferred to the amplitude of higher-order modes, whereas if the modulation is very small, the TEM_{10} mode mainly contributes to the displacement signal. Therefore, the displacement measurement is based on extracting the TEM_{10} mode component from the displaced TEM_{00} mode. There are two conventional ways to detect the displacement, i.e., split detection and TEM_{10} homodyne detection. The advances in both schemes are reviewed below.

One way to measure the displacement of a laser beam based on split photodetectors uses the two-pixel detector. In 2000, Fabre *et al.* proposed that the minimum measurable displacement D_{QNL} in a two-pixel detector by a TEM_{00} Gaussian beam is defined by [55]

$$D_{\mathrm{QNL}} = \sqrt{\frac{\pi}{8}}\frac{w_0}{\sqrt{N_{\mathrm{tot}}}}, \tag{5}$$

which is degraded in comparison to Eq. (4). This reduction arises from the mismatch between the noise mode of the split detection (i.e., the "flipped" mode) and the TEM_{10} mode introduced by displacement. To further enhance the sensitivity in split detection, one needs to fill the input beam with a squeezed noise mode, specifically, a squeezed "flipped" mode.

In 2002, Treps *et al.* used a spatial squeezed state for the displacement measurement and achieved a sub-QNL sensitivity [10]. They combined a 3.5-dB squeezed-vacuum TEM_{00} mode generated by an OPA cavity and its coherent "flipped" mode. Introducing a small transverse displacement modulation by two electro-optic modulators (EOMs) [Fig. 6(a)], they reduced the noise floor to a level of about 2.4 dB below the QNL. In 2003, they extended their work to measure two-dimensional sub-QNL displacements using a three-mode nonclassical state, which was generated by coupling three orthogonal transverse modes, two in a squeezed-vacuum state and one in a bright coherent field [Fig. 6(b)] [34]. In this experiment, they simultaneously achieved a 3.05 ± 0.1 dB horizontal noise reduction and a 2.0 ± 0.1 dB vertical noise reduction, with the smallest displacement detectable improved from 2.3 Å (1 Å = 0.1 nm) to 1.6 Å.

Another detection scheme, TEM_{10} homodyne detection, can achieve QNL for very small displacements [78]. This scheme uses a homodyne detection setup involving a TEM_{10} mode of the LO (Fig. 7). The noise mode of this detection is the

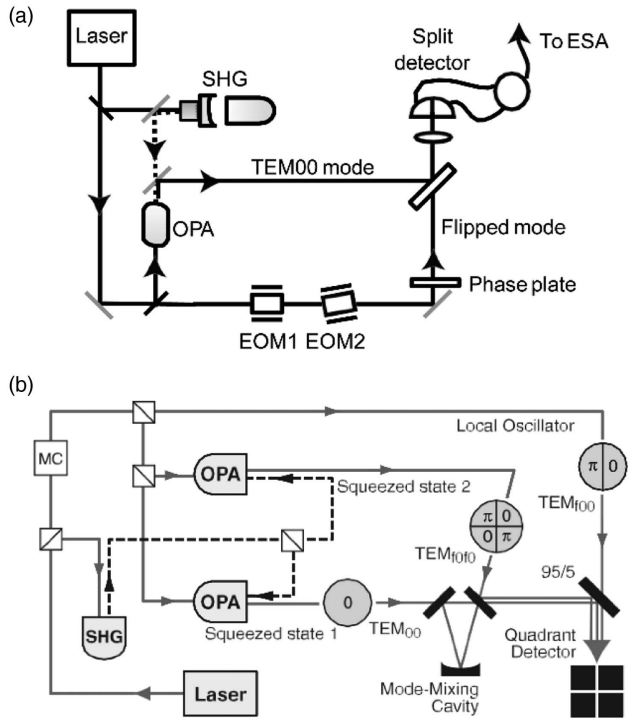

Fig. 6. (a) Scheme of the experiment setup in one-dimensional displacement measurement. Adapted with permission from Ref. [10]. (b) Scheme of the experiment setup in two-dimensional displacement measurement. The two squeezed modes are generated from two OPA cavities and mixed in a mode-mixing cavity. SHG, second harmonic generator; OPA, optical parametric amplifier; EOM, electro-optic modulator; ESA, electronic spectrum analyzer. Adapted with permission from Ref. [34].

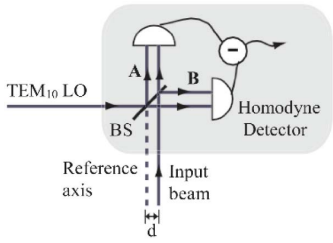

Fig. 7. TEM_{10} homodyne detection for beam displacement measurement. BS, 50/50 beam splitter; LO, local oscillator. The dashed line delineates the small displacement. Adapted with permission from Ref. [78].

TEM_{10} mode, which perfectly matches the information to be extracted, thereby accounting for its 100% efficiency detection in theory.

In this scheme, filling the input beam with a squeezed-vacuum TEM_{10} mode enables measurements beyond the QNL, which outperforms the split detection for equal values of squeezing. In 2006, Delaubert *et al.* [79] achieved a 2-dB enhancement in small displacement measurements using the TEM_{10} detection scheme. In 2014, Sun *et al.* [80] obtained 2.2 ± 0.2 dB spatial squeezing and reduced the minimum measurable displacement from 1.17 Å to 0.99 Å.

Measurements of rotation signals are similar to those of displacements and are also constrained by quantum mechanics; the rotation angle and angular momentum obey Heisenberg's uncertainty principle [81,82]. It is conventional to use a beam carrying orbital angular momentum such as the Laguerre–Gaussian modes [83] in spatial rotation measurements based on its vortex wavefront [84–86]. However, such measurement schemes are restricted to a resolution limit depending on the photon number and the orbital angular momentum of the beam [82]. Using nonclassical states such as the squeezed states of Laguerre–Gaussian modes can help beat such limits and reduce the noise below the SNL [87]. Liu *et al.* defined an n-order orbital angular position (OAP)-squeezed state, which is the combination of a bright $LG^{sin}_{0,n}$ mode coherent state and a squeezed-vacuum $LG^{sin}_{0,-n}$ state [87]. Using a first-order OAP-squeezed state in metrology, they achieved a 3-dB enhancement in rotation measurement over the QNL, with the sensitivity being improved from 24.9 nrad/$\sqrt{\text{Hz}}$ to 17.7 nrad/$\sqrt{\text{Hz}}$.

B. Optical Phase Estimation

Optical phase estimation (OPE), targeting quantum-limited precisions with limited photon numbers, is one of the key techniques in optical communications and precise metrology [88,89]. Adaptive homodyne measurement of an optical phase is an efficient and sophisticated method to approach an ideal canonical phase measurement [90,91]. If the adaptive control works properly, the sensitivity of the phase estimation is solely limited by the intrinsic phase uncertainty of the probe beam. Squeezed states [92,93] provide a further quantum enhancement in the phase estimations by suppressing quantum noise of the probe beams [94]. From theory, Wiseman *et al.* have demonstrated that an adaptive homodyne measurement with coherent states can estimate a fixed or time-varying optical phase with quantum-limited precision, and, moreover, it can be surpassed with the squeezed states [91,94,95]. In this section, we review how OPE provides an advance in sensitivity with the use of squeezed states.

The first experiment of a single-shot adaptive phase measurement was conducted by Armen *et al.* in 2002 [96]. They performed an adaptive homodyne measurement on weak coherent states with a fixed phase, and proved that the adaptive homodyne measurement can beat the heterodyne measurement in terms of phase estimation variances. Their system approached the intrinsic quantum uncertainty and paved the way for squeezing-enhanced phase estimation experiments.

In 2015, Berni *et al.* demonstrated quantum-enhanced *ab initio* OPE with squeezed-vacuum states and a real-time Bayesian adaptive estimation algorithm [16]. They generated 5.69 ± 0.07 dB squeezed-vacuum states using a cavity-enhanced degenerate PDC. The input, a squeezed-vacuum state, underwent a fixed phase shift [Fig. 8(a)], which was then measured by homodyne detection. The LO of the homodyne detection was feedback-controlled based on Bayesian inference. The quantum Fisher information for a pure 6-dB squeezed-vacuum state [Fig. 8(b)] was larger than that for a coherent state within a specific range of phase shift, which indicates that for an optimal measurement this system has one certain phase operating point. They performed a pre-estimation using the initial measurement results to make a rough estimate of the phase with Bayesian

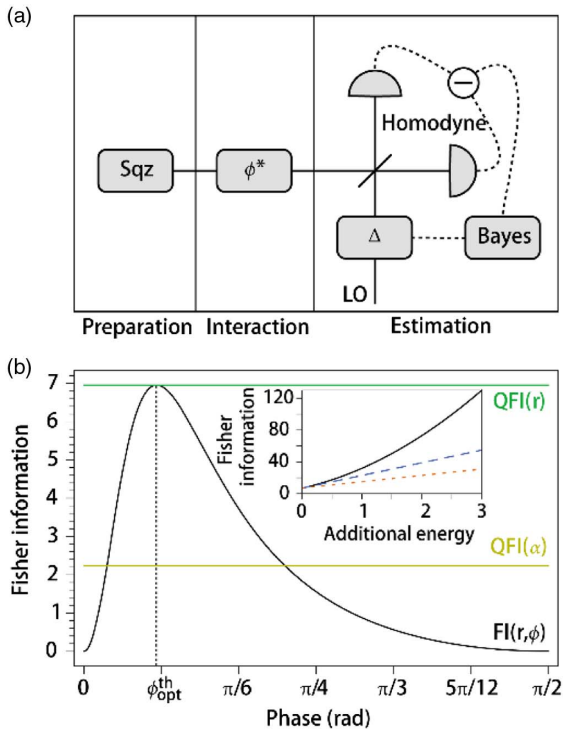

Fig. 8. (a) Schematic of squeezing-enhanced phase estimation. (b) Fisher information versus phase shift for a pure 6-dB squeezed-vacuum state. Adapted with permission from Ref. [16].

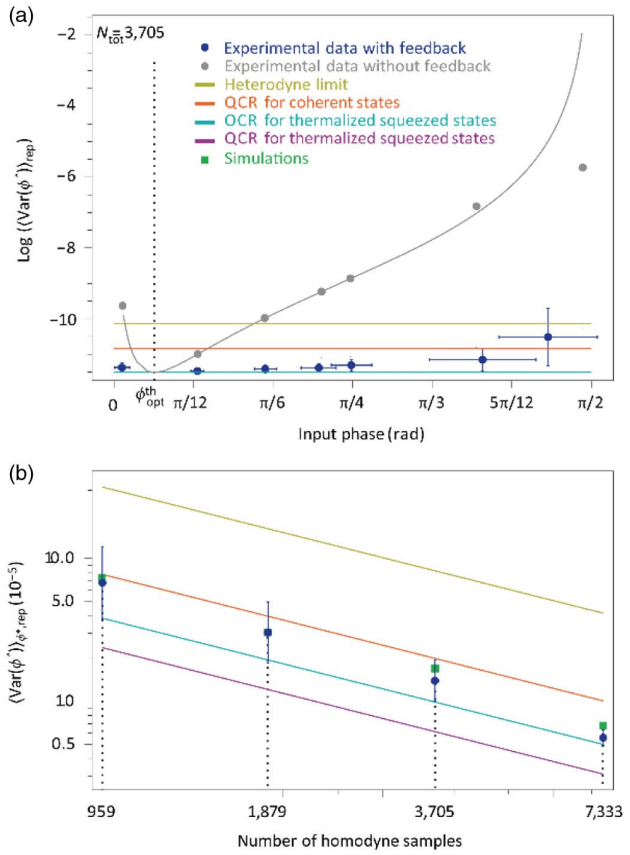

Fig. 9. (a) Dependence of estimation variance on input phase. (b) Dependence of estimation variance on the number of homodyne samples. Adapted with permission from Ref. [16].

inference. This information was used to shift the LO to the nearest optimal phase operating point, and then they measured the homodyne outcomes with a larger number of samples to obtain the final estimate. The estimation variances versus the different input phases and the number of homodyne samples (Fig. 9) show that adaptive-feedback control with squeezing enhancement outperforms the quantum Cramer–Rao bound (QCRB) for coherent states and approaches the optimal CRB for squeezed states.

Like single-shot phase estimations, time-varying phase estimations have also been investigated. In 2010, Wheatley *et al.* demonstrated a continuous adaptive phase measurement of a stochastically varying optical phase of coherent states, which provided better precision than the standard (non-adaptive) quantum limit [97]. They used real-time filtering and post-processed smoothing with an improvement of 2.24 ± 0.14 in terms of mean square error (MSE) compared with the standard quantum limit.

In 2012, squeezing-enhanced time-varying OPEs were realized by Yonezawa *et al.* [12]. They used a phase-squeezed state to track a time-varying optical phase with a range of approximately ± 1 radian. The phase-squeezed states were prepared by an OPO (Fig. 10) and modulated with a stochastically varying signal. The modulated phase-squeezed beams were detected by adaptive homodyne detection with an overall efficiency of 85%. A Kalman filter was used to design the phase-locked loop to track the stochastically varying optical phase. The phase tracking results (Fig. 11) show that there exists an optimum squeezing level in terms of MSE of the estimate. This is

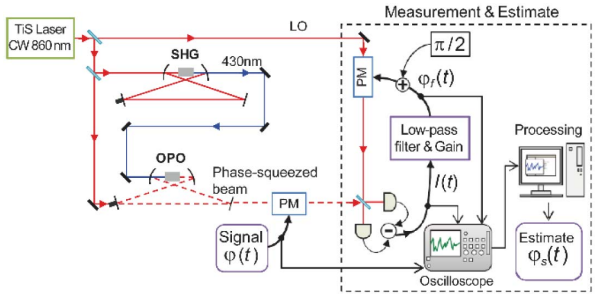

Fig. 10. Quantum-enhanced homodyne phase tracking system. Adapted with permission from Ref. [12].

because increasing anti-squeezing affects the precision of the estimate. With the optimal squeezing level, the MSEs [red crosses in Fig. 11(b)] were below the coherent-state limit [trace (i)]; quantum-enhanced phase tracking was realized with large phase changes.

Optical phase tracking with squeezing enhancement has a variety of applications, one of which is optomechanical motion sensing. Iwasawa *et al.* have worked on measuring the motion of a mirror under an external stochastic force using optical phase tracking techniques (Fig. 12) [98]. They estimated the position, momentum, and force of the mirror with optical

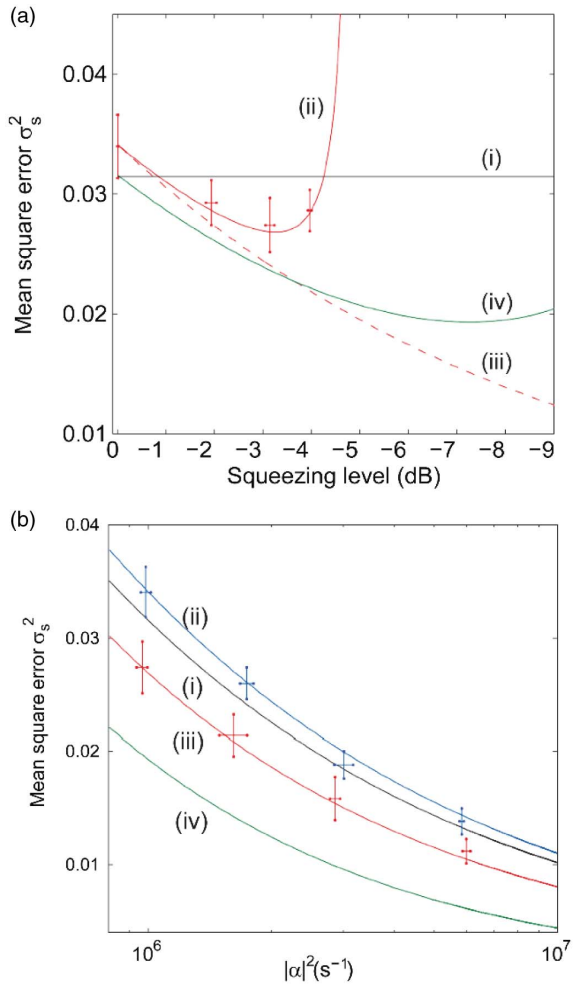

Fig. 11. (a) Dependence of MSE on squeezing level. (b) Dependence of MSE on amplitude squared $|\alpha|^2$. Adapted with permission from Ref. [12].

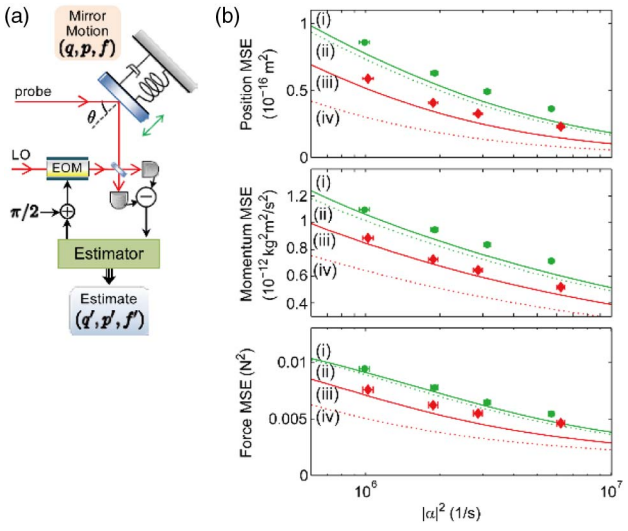

Fig. 12. (a) Schematic of the mirror-motion estimation and (b) dependence of MSE on amplitude squared $|\alpha|^2$. Adapted with permission from Ref. [98].

probe beams in coherent and phase-squeezed states. The estimations with coherent states [Fig. 12(b), green circles in right panel] were nearly reaching the coherent QCRB [trace (ii)]. The estimations with squeezed states (red diamonds) showed a clear enhancement and beat the coherent QCRB, although the estimation precisions did not reach the squeezed-state QCRB [trace (iv)] because of the impurity of the squeezed state. These results demonstrate the potential of the squeezing-enhanced phase estimation method for future quantum metrological applications.

C. Magnetic Field Measurement

Ultrasensitive magnetometers have found versatile applications, from geomagnetic field detection [99] to GW detection [100], nuclear-magnetic-resonance signal detection [101] to biomagnetism [102]. In 1992, Kupriyanov *et al.* proposed using squeezed light to detect magnetic fields [103]. Subsequently, many methods incorporating squeezed light have been reported to enhance the SNR, including quantum non-demolition detection, the quantum Kalman algorithm, and spin-squeezed atom ensembles, with the potential to reduce noise to the Heisenberg limit [104–108]. This section mainly covers sub-SNL magnetometers using polarization-squeezed light.

The nonlinear magneto-optical rotation (NMOR)-based magnetometer [109] is a common type of atomic optical magnetometer. It consists of a polarization interferometer where the polarization rotator is replaced by a well-prepared atomic ensemble [Fig. 5(a)], for example, a spin-oriented atom ensemble (Fig. 13) [108,110,111]. In this system, the polarization of the probe beam rotates under a weak external magnetic field because of the interaction between the probe beam and the atoms. According to Heisenberg's uncertainty principle, this magnetometer is ultimately confined by quantum noise including atomic projection noise and optical shot noise. A polarization-squeezed state of light can improve the performance of NMOR magnetometer.

Generally, the noise var(S_2^{out}) detected by an NMOR-based magnetometer is [11,112]

$$\text{var}(S_2^{\text{out}}) = \text{var}(S_2^{\text{in}}) + G^2 \frac{N_{\text{tot}}^2}{4} \text{var}(F_z), \tag{6}$$

where F_z denotes the collective atomic spins in the z direction, S represents the Stokes operators, G is the interaction strength,

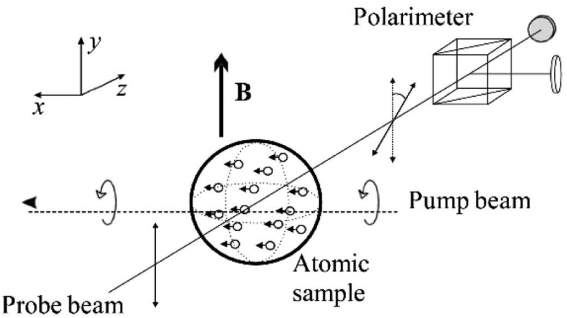

Fig. 13. Example of a prepared-atom ensemble where the pump beam orients the spins of the ensemble. The pump beam, probe beam, and magnetic field are mutually orthogonal. Adapted with permission from Ref. [108].

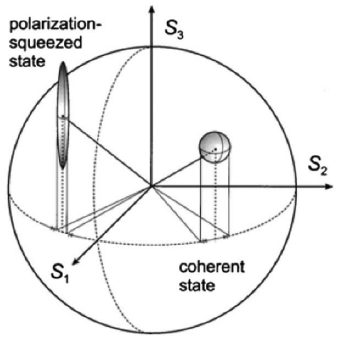

Fig. 14. Representation of quantum polarization states of bright coherent and bright amplitude-squeezed light on the Poincare sphere. Adapted with permission from Ref. [114].

and N_{tot} is the total number of photons. The optical shot noise and the atomic projection noise are described by $\text{var}(S_2^{\text{in}})$ and $\text{var}(F_z)$, respectively. In regard to the optical noise, the fluctuation of a bright coherent beam is depicted as a sphere of uncertainty on the surface of the Poincare sphere, whereas, for the S_2^{in} parameter, squeezed polarized light is represented by an ellipsoid [113,114] (Fig. 14). In this sense, the optical noise can be reduced by injecting a polarization-squeezed beam; therefore, a sub-QNL magnetometer can be built. The polarization-squeezed probe beam of such a magnetometer can be produced by mixing a squeezed vacuum with a coherent beam in a polarization beam splitter [11].

In 2010, Wolfgramm *et al.* used 3.6-dB polarization-squeezed light by mixing a vertically polarized vacuum-squeezed beam and a horizontally polarized LO to probe a hot unpolarized ensemble of rubidium atoms. They improved the sensitivity by 3.2 dB beyond the SNL [11]. In 2012, Horrom *et al.* enhanced the sensitivity to 1 $\text{pT}/\sqrt{\text{Hz}}$ in a sub-kilohertz frequency band using 2-dB low-frequency squeezed light generated by an atomic squeezer [115]. In 2014, Otterstrom *et al.* combined the squeezer and the magnetometry together, producing an *in situ* NMOR-based magnetometer [15]. In this experiment, they generated two-mode relative-intensity squeezed states via FWM obtaining an enhancement in sensitivity from 33.2 $\text{pT}/\sqrt{\text{Hz}}$ to 19.3 $\text{pT}/\sqrt{\text{Hz}}$. In 2016, Lucivero *et al.* achieved 1.5-dB noise suppression in a high atomic density ($n \approx 1.3 \times 10^{13}$ cm^{-3}) system [116].

D. Detection of Gravitational Waves

GWs propagating at the speed of light are generated by accelerated mass distributions, such as coalescing binary black holes and neutron stars [117]. Several initial detectors, such as LIGO, Virgo, GEO 600, and TAMA 300, made joint observations from 2002 to 2011 and have evolved into a global network [38]. In 2015, Advanced LIGO first observed a GW from a binary black-hole merger [118], the event symbolizing a new era in GW astronomy. In 2017, a GW from a binary black-hole coalescence was first detected by a three-detector observation, i.e., Advanced LIGO and Advanced Virgo [119]. In this section, we review the principle of Advanced LIGO and the squeezing-enhanced interferometer of LIGO.

Advanced LIGO consists of two similar kilometer-scale Michelson interferometers, located in Hanford and Livingston, U.S. [Fig. 15(a)]. When a GW passes through the two interferometers, the two arms of each interferometer are strained weakly, leading to a change in length [73]. This small change in length is converted to a weak phase signal between the two arms of each interferometer. The interferometers operate close to a dark fringe, which is the most sensitive point for GW detection. The light sources are 1064 nm wavelength Nd:YAG lasers, stabilized in intensity, frequency, and beam geometry. To detect the weak GW signal, enlarging the light power and suppressing noise are necessary. In the interferometer, arm cavities and power recycling cavity are used to increase the light power [120], and a partially transmitting signal-recycling mirror at the output is used to optimize signal extraction [121,122]. Moreover, the BS and arm cavities are all suspended as pendula on a seismic isolation platform. The optical path must be in vacuum to prevent phase fluctuations caused by Rayleigh scattering [14]. Figure 15(b) shows the sensitivity versus frequency of Advanced LIGO.

Although a GW has been detected, higher sensitivity and a broader frequency range are needed for future GW astronomy. Injecting nonclassical light is one powerful method for improvements, and squeezed light is the optimal choice [123]. A squeezing of 10 dB amounts to a 10-fold increase in light power, without introducing thermal deformation of the sensitivity from a high light power [124]. After proof-of-principle experiments [38,71,72], squeezed light was demonstrated in the GEO 600 [35] and LIGO [14] with sensitivity improvements.

The LIGO device with squeezing injection (Fig. 16) has a light source (H1 laser), Nd:YAG laser stabilized in frequency and intensity, emitting a 15 W light beam to a Michelson interferometer. The light in the arm cavities is power-enhanced to about 40 kW by the cavities. The interferometer operates close to a dark fringe, outputting light of about 30 mW power to the antisymmetric port. After going through the output Faraday isolator, a squeezed-vacuum state enters the interferometer from the antisymmetric port replacing the vacuum state. The vacuum-squeezed state is produced using PDC in a PPKTP crystal placed in an OPO cavity. To control the squeezing angle, a frequency-shifted laser beam is also sent through the interferometer, together with the squeezed-vacuum state. Before final detection, an output mode cleaner is used to filter out the frequency-shifted laser beam, where the squeezed

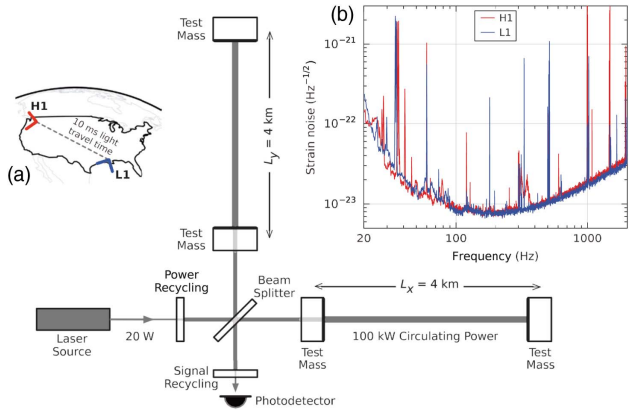

Fig. 15. (a) Simplified layout of Advanced LIGO. (b) Strain noise of each detector of Advanced LIGO. Adapted with permission from Ref. [118].

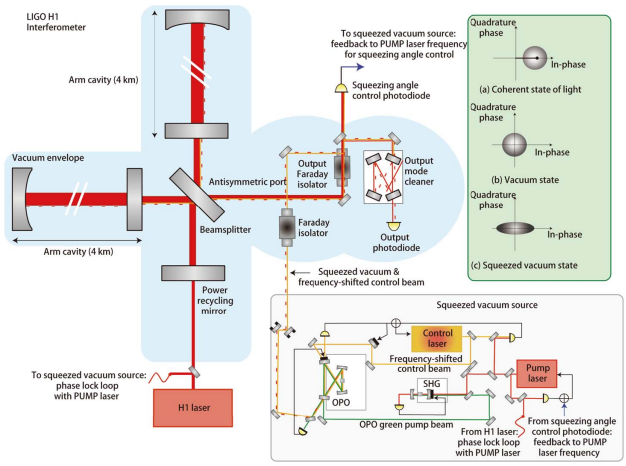

Fig. 16. Simplified setup of the H1 interferometer with vacuum-squeezed-state injection. Adapted with permission from Ref. [14].

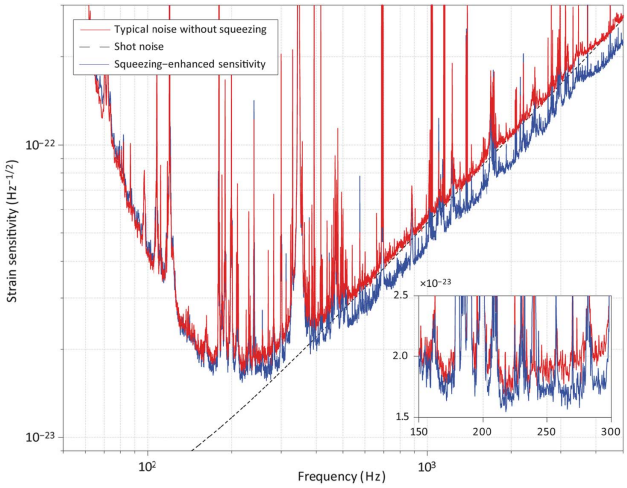

Fig. 17. Strain sensitivity of H1 detector with and without squeezed-vacuum injection. Adapted with permission from Ref. [14].

vacuum passes. For enhancing sensitivity and mitigating noise from the squeezed source, mode match between the squeezing and coherent states is needed in addition to critically controlling the squeezing angle and reducing the back-scattered light from the OPO cavity and the total loss in detection [14].

By injecting a ∼10-dB squeezed-vacuum state, the sensitivity improvement is up to 2.15 dB in the shot-noise-limited frequency band down to 150 Hz (Fig. 17). In addition, frequency-dependent squeezing [125,126] and two-mode squeezing were proposed [127] in optimizing GW detection in practice.

E. Fiber-Optic Sensing

Fiber interferometers are widely used in high-sensitivity strain sensors [128], fiber-optic gyroscopes [129], and quantum state detections [130], because fiber systems have unparalleled advantages such as immunity to electromagnetic disturbances, flexible multiplexing, and long-distance sensing [131,132]. We review next those experiments using fiber interferometer with squeezed-light injection.

As stated in the previous section, when N classical probes are used, the sensitivity of the optical measurement device is fundamentally limited by the shot noise. This precision can be surpassed using squeezed states. In a fiber system, the most challenging part for squeezing applications is the optical loss introduced by the fiber interferometer from decoherence effects and degradation of the squeezing factor [36]. Moreover, although squeezed states at high frequencies (MHz) are easy to achieve, they are not compatible with fiber sensing because the parameters to be measured for fiber position and strain sensing systems typically vary in the kilohertz frequency band [37]. To make full use of the squeezed state in fiber interferometers, many techniques have been developed, and a series of experiments has demonstrated the feasibility of quantum-enhanced fiber sensing [36,37,133,134].

In 2010, Mehmet *et al.* [36] first applied squeezed states in fiber-based Sagnac interferometers and realized sensitivities beyond SNL. A 10 m long fiber Sagnac interferometer was constructed and operated with a continuous-wave laser operating at 1550 nm wavelength, for which low-loss fibers are available. To compensate for the strong divergence and to minimize coupling loss, aspheric lenses and antireflecting coatings were used, and the modes of the two beams were carefully matched. The single-path transmission was 98% for these fiber-based Sagnac systems. The squeezed vacuum was injected in the unused port of the interferometer, and a noise reduction of 4.5 dB was achieved. When a 6 MHz phase modulation signal was added (Fig. 18), the results performed by BHD showed that the SNR with squeezed-light injection [Fig. 18, trace (a)] outperforms the SNR with vacuum state injection [Fig. 18, trace (b)].

In addition to high-frequency quantum-enhanced measurements in Sagnac interferometers being realized in fiber systems, a squeezing-enhanced fiber MZI for low-frequency phase measurement has also been demonstrated. In 2017, Liu *et al.* [37] reported a fiber MZI for phase measurements in the kilohertz frequency band beyond the SNL with a high-frequency (MHz range) squeezed state. The local light imported into one port of the interferometer was amplitude-modulated (AM) at the megahertz frequency to avoid low-frequency noise. Another input beam was the squeezed-vacuum field, which was generated by a NOPA and coupled to a polarization-maintaining fiber for quantum detection. The interference signal was then measured by BHD, and a 2-dB phase noise suppression below the SNL was achieved at a frequency of tens of kilohertz. Figure 19(a)

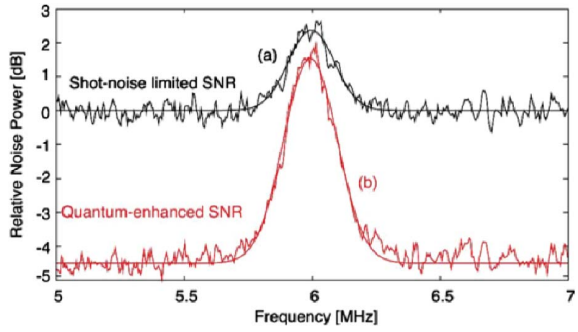

Fig. 18. Sagnac interferometer output signal. Adapted with permission from Ref. [36].

shows the phase noise reduction compared with shot noise at several frequencies; Figs. 19(b)–19(d) present experimental results obtained at 30 kHz, 80 kHz, and 150 kHz, respectively. With the injection of an AM coherent field and a squeezed state, the precision of the low-frequency phase measurement was enhanced and the noise reduction was independent of the modulation depth.

Apart from various fiber interferometers for phase measurements, adaptive homodyne systems have also been developed to estimate the phase signal in fiber systems. Not confined to measuring single frequency signals, in 2018, Zhang *et al.* designed a quantum-limited fiber homodyne system to detect low-frequency random phase signals beyond the π range [135]. They used a double sideband mode as a signal beam on which a random phase signal was imposed using a piezoelectric transducer. The signal was then detected with a homodyne detection system combined with two feedback loops, one working below 100 Hz to prevent the system from picking up ambient noise and the other serving as a Kalman filter to realize an optimal estimation. The optical parts were packed to minimize ambient noise, and all the optical components were polarization-maintaining fiber devices for a higher interferometer visibility in the fiber system. From phase tracking results (Fig. 20), they demonstrated quantum-limited fiber phase tracking over a large angular range at a photon flux of $\sim 10^6$. One can further improve such a system with a squeezed state of light.

These results in fiber interferometers open a door to real-world quantum communications and quantum sensing based on continuous-variable quantum optics [136,137].

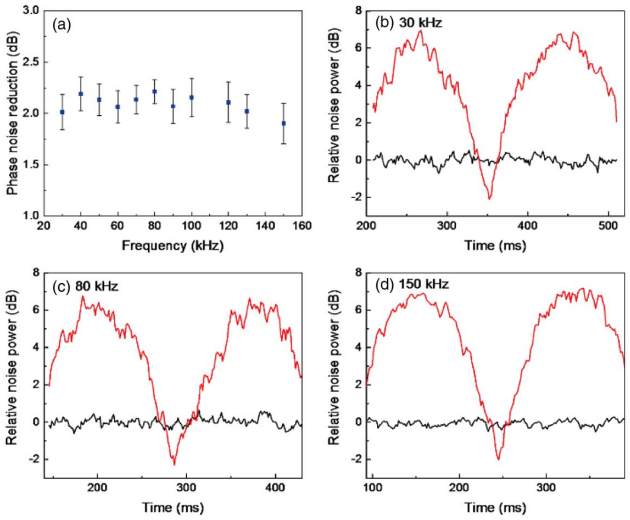

Fig. 19. (a) Dependence of phase noise reduction on frequency for the quantum-enhanced fiber interferometer. (b)–(d) Demodulated noise spectra of the interferometer output at 30 kHz, 80 kHz, and 150 kHz. Adapted with permission from Ref. [37].

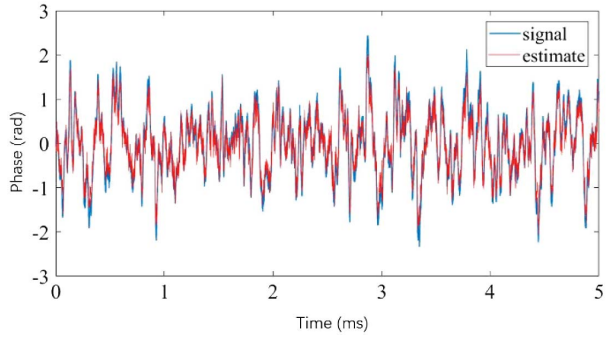

Fig. 20. Time domain results of fiber-optic phase tracking. Adapted with permission from Ref. [135].

4. PROSPECTS

Due to the rapid developments over the past 30 years, quantum squeezing has become much closer to practical applications than ever before. Stable squeezed-light sources above 10 dB are readily achievable in many quantum optic laboratories, and comparable squeezed-light sources are even commercially available now. The designs and configurations for different quantum-sensing systems are diversified according to the specific parameters to be measured. The techniques of signal processing and tracking have been greatly optimized to fully utilize the unique advantages of the available quantum squeezing. It should be noted that squeezed light at the current stage is still to be developed for further applications. For example, a robust squeezed source is required for certain applications under environmental disturbance. In addition, on-chip generation of high-quality squeezing is necessary for scalable quantum sensing in an integrated platform [26–30]. In this review, we have focused on several fields that are close to the practical utilizations of quantum-squeezed states of light. One can surely expect that many significant and practical applications are yet to appear. From this point of view, this review just serves as a starting point for stimulating future research on the sub-shot-noise measurement using quantum-squeezed states of light. One should not be surprised to see new applications of quantum-squeezed states in various frontier fields such as laser frequency stabilization [138], optic gyroscopes [139], frequency combs [140], and single-particle detection [141].

Funding. National Natural Science Foundation of China (NSFC) (11621091, 11874213, 61605072, 91636106); National Key R&D Program of China (2016YFA0302500, 2017YFA0303703); Australian Research Council (ARC) Centre of Excellence for Quantum Computation and Communication Technology (CE170100012).

REFERENCES

1. S. L. Braunstein and H. J. Kimble, "Teleportation of continuous quantum variables," Phys. Rev. Lett. **80**, 869–872 (1998).
2. A. Furusawa, J. L. Sørensen, S. L. Braunstein, C. A. Fuchs, H. J. Kimble, and E. S. Polzik, "Unconditional quantum teleportation," Science **282**, 706–709 (1998).
3. N. C. Menicucci, P. van Loock, M. Gu, C. Weedbrook, T. C. Ralph, and M. A. Nielsen, "Universal quantum computation with continuous-variable cluster states," Phys. Rev. Lett. **97**, 110501 (2006).
4. T. Aoki, G. Takahashi, T. Kajiya, J.-I. Yoshikawa, S. L. Braunstein, P. van Loock, and A. Furusawa, "Quantum error correction beyond qubits," Nat. Phys. **5**, 541–546 (2009).
5. M. Lassen, M. Sabuncu, A. Huck, J. Niset, G. Leuchs, N. J. Cerf, and U. L. Andersen, "Quantum optical coherence can survive photon

losses using a continuous-variable quantum erasure-correcting code," Nat. Photonics **4**, 700–705 (2010).
6. A. Ourjoumtsev, R. Tualle-Brouri, J. Laurat, and P. Grangier, "Generating optical Schrodinger kittens for quantum information processing," Science **312**, 83–86 (2006).
7. J. S. Neergaard-Nielsen, B. M. Nielsen, C. Hettich, K. Mølmer, and E. S. Polzik, "Generation of a superposition of odd photon number states for quantum information networks," Phys. Rev. Lett. **97**, 083604 (2006).
8. U. L. Andersen, J. S. Neergaard-Nielsen, P. van Loock, and A. Furusawa, "Hybrid discrete- and continuous-variable quantum information," Nat. Phys. **11**, 713–719 (2015).
9. M. I. Kolobov and C. Fabre, "Quantum limits on optical resolution," Phys. Rev. Lett. **85**, 3789–3792 (2000).
10. N. Treps, U. Andersen, B. Buchler, P. K. Lam, A. Maitre, H. A. Bachor, and C. Fabre, "Surpassing the standard quantum limit for optical imaging using nonclassical multimode light," Phys. Rev. Lett. **88**, 203601 (2002).
11. F. Wolfgramm, A. Cere, F. A. Beduini, A. Predojevic, M. Koschorreck, and M. W. Mitchell, "Squeezed-light optical magnetometry," Phys. Rev. Lett. **105**, 053601 (2010).
12. H. Yonezawa, D. Nakane, T. A. Wheatley, K. Iwasawa, S. Takeda, H. Arao, K. Ohki, K. Tsumura, D. W. Berry, T. C. Ralph, H. M. Wiseman, E. H. Huntington, and A. Furusawa, "Quantum-enhanced optical-phase tracking," Science **337**, 1514–1517 (2012).
13. M. A. Taylor, J. Janousek, V. Daria, J. Knittel, B. Hage, H.-A. Bachor, and W. P. Bowen, "Biological measurement beyond the quantum limit," Nat. Photonics **7**, 229–233 (2013).
14. The LIGO Scientific Collaboration, "Enhanced sensitivity of the LIGO gravitational wave detector by using squeezed states of light," Nat. Photonics **7**, 613–619 (2013).
15. N. Otterstrom, R. C. Pooser, and B. J. Lawrie, "Nonlinear optical magnetometry with accessible in situ optical squeezing," Opt. Lett. **39**, 6533–6536 (2014).
16. A. A. Berni, T. Gehring, B. M. Nielsen, V. Händchen, M. G. A. Paris, and U. L. Andersen, "*Ab initio* quantum-enhanced optical phase estimation using real-time feedback control," Nat. Photonics **9**, 577–581 (2015).
17. J. Liu, W. Liu, S. Li, D. Wei, H. Gao, and F. Li, "Enhancement of the angular rotation measurement sensitivity based on SU(2) and SU(1,1) interferometers," Photon. Res. **5**, 617–622 (2017).
18. L. A. Wu, H. J. Kimble, J. L. Hall, and H. Wu, "Generation of squeezed states by parametric down conversion," Phys. Rev. Lett. **57**, 2520–2523 (1986).
19. R. E. Slusher, L. W. Hollberg, B. Yurke, J. C. Mertz, and J. F. Valley, "Observation of squeezed states generated by four-wave mixing in an optical cavity," Phys. Rev. Lett. **55**, 2409–2412 (1985).
20. C. F. McCormick, A. M. Marino, V. Boyer, and P. D. Lett, "Strong low-frequency quantum correlations from a four-wave-mixing amplifier," Phys. Rev. A **78**, 043816 (2008).
21. Q. Glorieux, L. Guidoni, S. Guibal, J.-P. Likforman, and T. Coudreau, "Quantum correlations by four-wave mixing in an atomic vapor in a nonamplifying regime: quantum beam splitter for photons," Phys. Rev. A **84**, 053826 (2011).
22. D. Zhang, C. Li, Z. Zhang, Y. Zhang, Y. Zhang, and M. Xiao, "Enhanced intensity-difference squeezing via energy-level modulations in hot atomic media," Phys. Rev. A **96**, 043847 (2017).
23. M. Rosenbluh and R. M. Shelby, "Squeezed optical solitons," Phys. Rev. Lett. **66**, 153–156 (1991).
24. S. Schmitt, J. Ficker, M. Wolff, F. Konig, A. Sizmann, and G. Leuchs, "Photon-number squeezed solitons from an asymmetric fiber-optic Sagnac interferometer," Phys. Rev. Lett. **81**, 2446–2449 (1998).
25. R. Dong, J. Heersink, J. F. Corney, P. D. Drummond, U. L. Andersen, and G. Leuchs, "Experimental evidence for Raman-induced limits to efficient squeezing in optical fibers," Opt. Lett. **33**, 116–118 (2008).
26. A. H. Safavi-Naeini, S. Gröblacher, J. T. Hill, J. Chan, M. Aspelmeyer, and O. Painter, "Squeezed light from a silicon micromechanical resonator," Nature **500**, 185–189 (2013).
27. T. P. Purdy, P. L. Yu, R. W. Peterson, N. S. Kampel, and C. A. Regal, "Strong optomechanical squeezing of light," Phys. Rev. X **3**, 031012 (2013).
28. T. Boulier, M. Bamba, A. Amo, C. Adrados, A. Lemaitre, E. Galopin, I. Sagnes, J. Bloch, C. Ciuti, E. Giacobino, and A. Bramati, "Polariton-generated intensity squeezing in semiconductor micropillars," Nat. Commun. **5**, 3260 (2014).
29. A. Dutt, K. Luke, S. Manipatruni, A. L. Gaeta, P. Nussenzveig, and M. Lipson, "On-chip optical squeezing," Phys. Rev. Appl. **3**, 044005 (2015).
30. M. Stefszky, R. Ricken, C. Eigner, V. Quiring, H. Herrmann, and C. Silberhorn, "Waveguide cavity resonator as a source of optical squeezing," Phys. Rev. Appl. **7**, 044026 (2017).
31. S. Suzuki, H. Yonezawa, F. Kannari, M. Sasaki, and A. Furusawa, "7 dB quadrature squeezing at 860 nm with periodically poled $KTiOPO_4$," Appl. Phys. Lett. **89**, 061116 (2006).
32. H. Vahlbruch, M. Mehmet, S. Chelkowski, B. Hage, A. Franzen, N. Lastzka, S. Gossler, K. Danzmann, and R. Schnabel, "Observation of squeezed light with 10-dB quantum-noise reduction," Phys. Rev. Lett. **100**, 033602 (2008).
33. H. Vahlbruch, M. Mehmet, K. Danzmann, and R. Schnabel, "Detection of 15 dB squeezed states of light and their application for the absolute calibration of photoelectric quantum efficiency," Phys. Rev. Lett. **117**, 110801 (2016).
34. N. Treps, N. Grosse, W. P. Bowen, C. Fabre, H.-A. Bachor, and P. K. Lam, "A quantum laser pointer," Science **301**, 940–943 (2003).
35. The LIGO Scientific Collaboration, "A gravitational wave observatory operating beyond the quantum shot-noise limit," Nat. Phys. **7**, 962–965 (2011).
36. M. Mehmet, T. Eberle, S. Steinlechner, H. Vahlbruch, and R. Schnabel, "Demonstration of a quantum-enhanced fiber Sagnac interferometer," Opt. Lett. **35**, 1665–1667 (2010).
37. F. Liu, Y. Zhou, J. Yu, J. Guo, Y. Wu, S. Xiao, D. Wei, Y. Zhang, X. Jia, and M. Xiao, "Squeezing-enhanced fiber Mach-Zehnder interferometer for low-frequency phase measurement," Appl. Phys. Lett. **110**, 021106 (2017).
38. K. Goda, O. Miyakawa, E. E. Mikhailov, S. Saraf, R. Adhikari, K. McKenzie, R. Ward, S. Vass, A. J. Weinstein, and N. Mavalvala, "A quantum-enhanced prototype gravitational-wave detector," Nat. Phys. **4**, 472–476 (2008).
39. Z. Qin, L. Cao, H. Wang, A. M. Marino, W. Zhang, and J. Jing, "Experimental generation of multiple quantum correlated beams from hot rubidium vapor," Phys. Rev. Lett. **113**, 023602 (2014).
40. G. Abdisa, I. Ahmed, X. Wang, Z. Liu, H. Wang, and Y. Zhang, "Controllable hybrid shape of correlation and squeezing," Phys. Rev. A **94**, 023849 (2016).
41. H. Chen, X. Zhang, D. Zhu, C. Yang, T. Jiang, H. Zheng, and Y. Zhang, "Dressed four-wave mixing second-order Talbot effect," Phys. Rev. A **90**, 043846 (2014).
42. Z. Y. Ou, S. F. Pereira, H. J. Kimble, and K. C. Peng, "Realization of the Einstein-Podolsky-Rosen paradox for continuous variables," Phys. Rev. Lett. **68**, 3663–3666 (1992).
43. X. Su, Y. Zhao, S. Hao, X. Jia, C. Xie, and K. Peng, "Experimental preparation of eight-partite cluster state for photonic qumodes," Opt. Lett. **37**, 5178–5180 (2012).
44. V. Boyer, A. M. Marino, R. C. Pooser, and P. D. Lett, "Entangled images from four-wave mixing," Science **321**, 544–547 (2008).
45. M. Lassen, G. Leuchs, and U. L. Andersen, "Continuous variable entanglement and squeezing of orbital angular momentum states," Phys. Rev. Lett. **102**, 163602 (2009).
46. J. Janousek, K. Wagner, J. F. Morizur, N. Treps, P. K. Lam, C. C. Harb, and H. A. Bachor, "Optical entanglement of co-propagating modes," Nat. Photonics **3**, 399–402 (2009).
47. J. Roslund, R. M. de Araújo, S. Jiang, C. Fabre, and N. Treps, "Wavelength-multiplexed quantum networks with ultrafast frequency combs," Nat. Photonics **8**, 109–112 (2014).
48. M. Chen, N. C. Menicucci, and O. Pfister, "Experimental realization of multipartite entanglement of 60 modes of a quantum optical frequency comb," Phys. Rev. Lett. **112**, 120505 (2014).
49. S. Gerke, J. Sperling, W. Vogel, Y. Cai, J. Roslund, N. Treps, and C. Fabre, "Full multipartite entanglement of frequency-comb Gaussian states," Phys. Rev. Lett. **114**, 050501 (2015).
50. S. Yokoyama, R. Ukai, S. C. Armstrong, C. Sornphiphatphong, T. Kaji, S. Suzuki, J.-I. Yoshikawa, H. Yonezawa, N. C. Menicucci, and A. Furusawa, "Ultra-large-scale continuous-variable cluster states multiplexed in the time domain," Nat. Photonics **7**, 982–986 (2013).

51. C. Gabriel, A. Aiello, W. Zhong, T. G. Euser, N. Y. Joly, P. Banzer, M. Fortsch, D. Elser, U. L. Andersen, C. Marquardt, P. S. Russell, and G. Leuchs, "Entangling different degrees of freedom by quadrature squeezing cylindrically polarized modes," Phys. Rev. Lett. **106**, 060502 (2011).
52. K. Liu, J. Guo, C. Cai, S. Guo, and J. Gao, "Experimental generation of continuous-variable hyperentanglement in an optical parametric oscillator," Phys. Rev. Lett. **113**, 170501 (2014).
53. A. S. Coelho, F. A. S. Barbosa, K. N. Cassemiro, A. S. Villar, M. Martinelli, and P. Nussenzveig, "Three-color entanglement," Science **326**, 823–826 (2009).
54. F. A. S. Barbosa, A. S. Coelho, L. F. Muñoz-Martínez, L. Ortiz-Gutiérrez, A. S. Villar, P. Nussenzveig, and M. Martinelli, "Hexapartite entanglement in an above-threshold optical parametric oscillator," Phys. Rev. Lett. **121**, 073601 (2018).
55. C. Fabre, J. B. Fouet, and A. Maître, "Quantum limits in the measurement of very small displacements in optical images," Opt. Lett. **25**, 76–78 (2000).
56. B. Yurke, S. L. McCall, and J. R. Klauder, "SU(2) and SU(1,1) interferometers," Phys. Rev. A **33**, 4033–4054 (1986).
57. M. J. Holland and K. Burnett, "Interferometric detection of optical phase shifts at the Heisenberg limit," Phys. Rev. Lett. **71**, 1355–1358 (1993).
58. G. M. D'Ariano and M. F. Sacchi, "Two-mode heterodyne phase detection," Phys. Rev. A **52**, R4309–R4312 (1995).
59. B. L. Higgins, D. W. Berry, S. D. Bartlett, H. M. Wiseman, and G. J. Pryde, "Entanglement-free Heisenberg-limited phase estimation," Nature **450**, 393–396 (2007).
60. I. Afek, O. Ambar, and Y. Silberberg, "High-NOON states by mixing quantum and classical light," Science **328**, 879–881 (2010).
61. Z. Y. Ou, "Enhancement of the phase-measurement sensitivity beyond the standard quantum limit by a nonlinear interferometer," Phys. Rev. A **85**, 023815 (2012).
62. F. Hudelist, J. Kong, C. Liu, J. Jing, Z. Y. Ou, and W. Zhang, "Quantum metrology with parametric amplifier-based photon correlation interferometers," Nat. Commun. **5**, 3049 (2014).
63. D. F. Walls, "Squeezed states of light," Nature **306**, 141–146 (1983).
64. G. J. Milburn, M. D. Levenson, R. M. Shelby, S. H. Perlmutter, R. G. Devoe, and D. F. Walls, "Optical-fiber media for squeezed-state generation," J. Opt. Soc. Am. B **4**, 1476–1489 (1987).
65. S. F. Pereira, M. Xiao, H. J. Kimble, and J. L. Hall, "Generation of squeezed light by intracavity frequency doubling," Phys. Rev. A **38**, 4931–4934 (1988).
66. W. H. Richardson, S. Machida, and Y. Yamamoto, "Squeezed photon-number noise and sub-Poissonian electrical partition noise in a semiconductor laser," Phys. Rev. Lett. **66**, 2867–2870 (1991).
67. Y. Takeno, M. Yukawa, H. Yonezawa, and A. Furusawa, "Observation of –9 dB quadrature squeezing with improvement of phase stability in homodyne measurement," Opt. Express **15**, 4321–4327 (2007).
68. J. Bauchrowitz, T. Westphal, and R. Schnabel, "A graphical description of optical parametric generation of squeezed states of light," Am. J. Phys. **81**, 767–771 (2013).
69. G. Breitenbach, S. Schiller, and J. Mlynek, "Measurement of the quantum states of squeezed light," Nature **387**, 471–475 (1997).
70. C. M. Caves, "Quantum-mechanical noise in an interferometer," Phys. Rev. D **23**, 1693–1708 (1981).
71. M. Xiao, L. A. Wu, and H. J. Kimble, "Precision measurement beyond the shot-noise limit," Phys. Rev. Lett. **59**, 278–281 (1987).
72. P. Grangier, R. E. Slusher, B. Yurke, and A. LaPorta, "Squeezed-light-enhanced polarization interferometer," Phys. Rev. Lett. **59**, 2153–2156 (1987).
73. A. Abramovici, W. E. Althouse, R. W. P. Drever, Y. Gürsel, S. Kawamura, F. J. Raab, D. Shoemaker, L. Sievers, R. E. Spero, K. S. Thorne, R. E. Vogt, R. Weiss, S. E. Whitcomb, and M. E. Zucker, "LIGO: the laser interferometer gravitational-wave observatory," Science **256**, 325–333 (1992).
74. Y. Q. Li, P. Lynam, M. Xiao, and P. J. Edwards, "Sub-shot-noise laser Doppler anemometry with amplitude-squeezed light," Phys. Rev. Lett. **78**, 3105–3108 (1997).
75. C. A. J. Putman, B. G. De Grooth, N. F. Van Hulst, and J. Greve, "A detailed analysis of the optical beam deflection technique for use in atomic force microscopy," J. Appl. Phys. **72**, 6–12 (1992).
76. A. C. Boccara, D. Fournier, and J. Badoz, "Thermo-optical spectroscopy: detection by the 'mirage effect'," Appl. Phys. Lett. **36**, 130–132 (1980).
77. J. W. Tay, M. T. L. Hsu, and W. P. Bowen, "Quantum limited particle sensing in optical tweezers," Phys. Rev. A **80**, 063806 (2009).
78. T. L. H. Magnus, D. Vincent, L. Ping Koy, and P. B. Warwick, "Optimal optical measurement of small displacements," J. Opt. B **6**, 495–501 (2004).
79. V. Delaubert, N. Treps, M. Lassen, C. C. Harb, C. Fabre, P. K. Lam, and H. A. Bachor, "TEM_{10} homodyne detection as an optimal small-displacement and tilt-measurement scheme," Phys. Rev. A **74**, 053823 (2006).
80. H.-X. Sun, Z.-L. Liu, K. Liu, R.-G. Yang, J.-X. Zhang, and J.-R. Gao, "Experimental demonstration of a displacement measurement of an optical beam beyond the quantum noise limit," Chin. Phys. Lett. **31**, 084202 (2014).
81. S. M. Barnett and D. T. Pegg, "Quantum theory of rotation angles," Phys. Rev. A **41**, 3427–3435 (1990).
82. S. M. Barnett and R. Zambrini, "Resolution in rotation measurements," J. Mod. Opt. **53**, 613–625 (2006).
83. L. Allen, M. W. Beijersbergen, R. J. C. Spreeuw, and J. P. Woerdman, "Orbital angular momentum of light and the transformation of Laguerre-Gaussian laser modes," Phys. Rev. A **45**, 8185–8189 (1992).
84. J. Courtial, K. Dholakia, D. A. Robertson, L. Allen, and M. J. Padgett, "Measurement of the rotational frequency shift imparted to a rotating light beam possessing orbital angular momentum," Phys. Rev. Lett. **80**, 3217–3219 (1998).
85. M. P. J. Lavery, F. C. Speirits, S. M. Barnett, and M. J. Padgett, "Detection of a spinning object using light's orbital angular momentum," Science **341**, 537–540 (2013).
86. S. Xiao, L. Zhang, D. Wei, F. Liu, Y. Zhang, and M. Xiao, "Orbital angular momentum-enhanced measurement of rotation vibration using a Sagnac interferometer," Opt. Express **26**, 1997–2005 (2018).
87. K. Liu, C. X. Cai, J. Li, L. Ma, H. X. Sun, and J. R. Gao, "Squeezing-enhanced rotating-angle measurement beyond the quantum limit," Appl. Phys. Lett. **113**, 261103 (2018).
88. V. Giovannetti, S. Lloyd, and L. Maccone, "Advances in quantum metrology," Nat. Photonics **5**, 222–229 (2011).
89. J. P. Dowling and K. P. Seshadreesan, "Quantum optical technologies for metrology, sensing, and imaging," J. Lightwave Technol. **33**, 2359–2370 (2015).
90. H. M. Wiseman, "Adaptive phase measurements of optical modes: going beyond the marginal *Q* distribution," Phys. Rev. Lett. **75**, 4587–4590 (1995).
91. D. T. Pope, H. M. Wiseman, and N. K. Langford, "Adaptive phase estimation is more accurate than nonadaptive phase estimation for continuous beams of light," Phys. Rev. A **70**, 043812 (2004).
92. G. Masada, "Current development of experimental investigation of squeezed light and its applications," Proc. SPIE **9269**, 92690B (2014).
93. U. L. Andersen, T. Gehring, C. Marquardt, and G. Leuchs, "30 years of squeezed light generation," Phys. Scr. **91**, 053001 (2016).
94. D. W. Berry and H. M. Wiseman, "Adaptive phase measurements for narrowband squeezed beams," Phys. Rev. A **73**, 063824 (2006).
95. D. W. Berry and H. M. Wiseman, "Adaptive quantum measurements of a continuously varying phase," Phys. Rev. A **65**, 043803 (2002).
96. M. A. Armen, J. K. Au, J. K. Stockton, A. C. Doherty, and H. Mabuchi, "Adaptive homodyne measurement of optical phase," Phys. Rev. Lett. **89**, 133602 (2002).
97. T. Wheatley, D. Berry, H. Yonezawa, D. Nakane, H. Arao, D. Pope, T. Ralph, H. Wiseman, A. Furusawa, and E. Huntington, "Adaptive optical phase estimation using time-symmetric quantum smoothing," Phys. Rev. Lett. **104**, 093601 (2010).
98. K. Iwasawa, K. Makino, H. Yonezawa, M. Tsang, A. Davidovic, E. Huntington, and A. Furusawa, "Quantum-limited mirror-motion estimation," Phys. Rev. Lett. **111**, 163602 (2013).
99. D. Budker and M. Romalis, "Optical magnetometry," Nat. Phys. **3**, 227–234 (2007).
100. G. M. Harry, I. Jin, H. J. Paik, T. R. Stevenson, and F. C. Wellstood, "Two-stage superconducting-quantum-interference-device amplifier in a high-*Q* gravitational wave transducer," Appl. Phys. Lett. **76**, 1446–1448 (2000).

101. R. McDermott, A. H. Trabesinger, M. Mück, E. L. Hahn, A. Pines, and J. Clarke, "Liquid-state NMR and scalar couplings in microtesla magnetic fields," Science **295**, 2247–2249 (2002).
102. E. Rodriguez, N. George, J.-P. Lachaux, J. Martinerie, B. Renault, and F. J. Varela, "Perception's shadow: long-distance synchronization of human brain activity," Nature **397**, 430–433 (1999).
103. D. V. Kupriyanov and I. M. Sokolov, "Optical-detection of magnetic-resonance by classical and squeezed light," Quantum Opt. **4**, 55–70 (1992).
104. J. M. Geremia, J. K. Stockton, and H. Mabuchi, "Suppression of spin projection noise in broadband atomic magnetometry," Phys. Rev. Lett. **94**, 203002 (2005).
105. W. Wasilewski, K. Jensen, H. Krauter, J. J. Renema, M. V. Balabas, and E. S. Polzik, "Quantum noise limited and entanglement-assisted magnetometry," Phys. Rev. Lett. **104**, 133601 (2010).
106. J. M. Geremia, J. K. Stockton, A. C. Doherty, and H. Mabuchi, "Quantum Kalman filtering and the Heisenberg limit in atomic magnetometry," Phys. Rev. Lett. **91**, 250801 (2003).
107. A. Kuzmich, L. Mandel, and N. P. Bigelow, "Generation of spin squeezing via continuous quantum nondemolition measurement," Phys. Rev. Lett. **85**, 1594–1597 (2000).
108. M. Auzinsh, D. Budker, D. F. Kimball, S. M. Rochester, J. E. Stalnaker, A. O. Sushkov, and V. V. Yashchuk, "Can a quantum nondemolition measurement improve the sensitivity of an atomic magnetometer?" Phys. Rev. Lett. **93**, 173002 (2004).
109. H. C. Seton, J. M. S. Hutchison, and D. M. Bussell, "Liquid helium cryostat for SQUID-based MRI receivers," Cryogenics **45**, 348–355 (2005).
110. D. Budker, W. Gawlik, D. F. Kimball, S. M. Rochester, V. V. Yashchuk, and A. Weis, "Resonant nonlinear magneto-optical effects in atoms," Rev. Mod. Phys. **74**, 1153–1201 (2002).
111. D. Budker, V. Yashchuk, and M. Zolotorev, "Nonlinear magneto-optic effects with ultranarrow widths," Phys. Rev. Lett. **81**, 5788–5791 (1998).
112. M. Koschorreck, M. Napolitano, B. Dubost, and M. W. Mitchell, "Sub-projection-noise sensitivity in broadband atomic magnetometry," Phys. Rev. Lett. **104**, 093602 (2010).
113. W. P. Bowen, R. Schnabel, H.-A. Bachor, and P. K. Lam, "Polarization squeezing of continuous variable stokes parameters," Phys. Rev. Lett. **88**, 093601 (2002).
114. N. Korolkova, G. Leuchs, R. Loudon, T. C. Ralph, and C. Silberhorn, "Polarization squeezing and continuous-variable polarization entanglement," Phys. Rev. A **65**, 052306 (2002).
115. T. Horrom, R. Singh, J. P. Dowling, and E. E. Mikhailov, "Quantum-enhanced magnetometer with low-frequency squeezing," Phys. Rev. A **86**, 023803 (2012).
116. V. G. Lucivero, R. Jiménez-Martínez, J. Kong, and M. W. Mitchell, "Squeezed-light spin noise spectroscopy," Phys. Rev. A **93**, 053802 (2016).
117. A. Sandage, "The case for H0 roughly 55 from the 21 centimeter linewidth absolute magnitude relation for field galaxies," Astrophys. J. **331**, 605–619 (1988).
118. LIGO Scientific Collaboration and Virgo Collaboration, "Observation of gravitational waves from a binary black hole merger," Phys. Rev. Lett. **116**, 061102 (2016).
119. LIGO Scientific Collaboration and Virgo Collaboration, "GW170817: observation of gravitational waves from a binary neutron star inspiral," Phys. Rev. Lett. **119**, 161101 (2017).
120. R. W. P. Drever, J. Hought, A. J. Munley, S. A. Lee, R. Spero, S. E. Whitcomb, H. Ward, G. M. Ford, M. Hereld, N. A. Robertson, I. Kerr, J. R. Pugh, G. P. Newton, B. Meers, E. D. Brooks, and Y. Gursel, "Gravitational wave detectors using laser interferometers and optical cavities: ideas, principles and prospects," in *Quantum Optics, Experimental Gravity, and Measurement Theory*, P. Meystre and M. O. Scully, eds. (Springer, 1983), pp. 503–514.
121. B. J. Meers, "Recycling in laser-interferometric gravitational-wave detectors," Phys. Rev. D **38**, 2317–2326 (1988).
122. G. Heinzel, J. Mizuno, R. Schilling, W. Winkler, A. Rudiger, and K. Danzmann, "An experimental demonstration of resonant sideband extraction for laser-interferometric gravitational wave detectors," Phys. Lett. A **217**, 305–314 (1996).
123. R. Schnabel, "Squeezed states of light and their applications in laser interferometers," Phys. Rep. Rev. Sec. Phys. Lett. **684**, 1–51 (2017).
124. M. Punturo, M. Abernathy, F. Acernese, B. Allen, N. Andersson, K. Arun, F. Barone, B. Barr, M. Barsuglia, M. Beker, N. Beveridge, S. Birindelli, S. Bose, L. Bosi, S. Braccini, C. Bradaschia, T. Bulik, E. Calloni, G. Cella, E. C. Mottin, S. Chelkowski, A. Chincarini, J. Clark, E. Coccia, C. Colacino, J. Colas, A. Cumming, L. Cunningham, E. Cuoco, S. Danilishin, K. Danzmann, G. De Luca, R. De Salvo, T. Dent, R. Derosa, L. Di Fiore, A. Di Virgilio, M. Doets, V. Fafone, P. Falferi, R. Flaminio, J. Franc, F. Frasconi, A. Freise, P. Fulda, J. Gair, G. Gemme, A. Gennai, A. Giazotto, K. Glampedakis, M. Granata, H. Grote, G. Guidi, G. Hammond, M. Hannam, J. Harms, D. Heinert, M. Hendry, I. Heng, E. Hennes, S. Hild, J. Hough, S. Husa, S. Huttner, G. Jones, F. Khalili, K. Kokeyama, K. Kokkotas, B. Krishnan, M. Lorenzini, H. Luck, E. Majorana, I. Mandel, V. Mandic, I. Martin, C. Michel, Y. Minenkov, N. Morgado, S. Mosca, B. Mours, H. Muller-Ebhardt, P. Murray, R. Nawrodt, J. Nelson, R. Oshaughnessy, C. D. Ott, C. Palomba, A. Paoli, G. Parguez, A. Pasqualetti, R. Passaquieti, D. Passuello, L. Pinard, R. Poggiani, P. Popolizio, M. Prato, P. Puppo, D. Rabeling, P. Rapagnani, J. Read, T. Regimbau, H. Rehbein, S. Reid, L. Rezzolla, F. Ricci, F. Richard, A. Rocchi, S. Rowan, A. Rüdiger, B. Sassolas, B. Sathyaprakash, R. Schnabe, C. Schwarz, P. Seidel, A. Sintes, K. Somiya, F. Speirits, K. Strain, S. Strigin, P. Sutton, S. Tarabrin, J. van den Brand, C. van Leewen, M. van Vegge, C. van den Broeck, A. Vecchio, J. Veitch, F. Vetrano, A. Vicere, S. Vyatchanin, B. Willke, G. Woan, P. Wolfango, and K. Yamamoto, "The third generation of gravitational wave observatories and their science reach," Class. Quantum Gravity **27**, 084007 (2010).
125. H. J. Kimble, Y. Levin, A. B. Matsko, K. S. Thorne, and S. P. Vyatchanin, "Conversion of conventional gravitational-wave interferometers into quantum nondemolition interferometers by modifying their input and/or output optics," Phys. Rev. D **65**, 022002 (2001).
126. E. Oelker, T. Isogai, J. Miller, M. Tse, L. Barsotti, N. Mavalvala, and M. Evans, "Audio-band frequency-dependent squeezing for gravitational-wave detectors," Phys. Rev. Lett. **116**, 041102 (2016).
127. S. Steinlechner, J. Bauchrowitz, M. Meinders, H. Müller-Ebhardt, K. Danzmann, and R. Schnabel, "Quantum-dense metrology," Nat. Photonics **7**, 626–630 (2013).
128. G. Gagliardi, M. Salza, S. Avino, P. Ferraro, and P. De Natale, "Probing the ultimate limit of fiber-optic strain sensing," Science **330**, 1081–1084 (2010).
129. B. Culshaw, "The optical fibre Sagnac interferometer: an overview of its principles and applications," Meas. Sci. Technol. **17**, R1–R16 (2006).
130. C. Xia, D. Wang, Y. Wu, J. Guo, F. Liu, Y. Zhang, and M. Xiao, "Continuous-variable entanglement measurement using an unbalanced Mach-Zehnder interferometer," Opt. Lett. **40**, 1121–1124 (2015).
131. L. Mescia and F. Prudenzano, "Advances on optical fiber sensors," Fibers **2**, 1–23 (2014).
132. Y. Xu, P. Lu, L. Chen, and X. Bao, "Recent developments in microstructured fiber optic sensors," Fibers **5**, 3 (2017).
133. A. Luis, I. Morales, and Á. Rivas, "Nonlinear fiber gyroscope for quantum metrology," Phys. Rev. A **94**, 013830 (2016).
134. Z. Zhai and J. Gao, "Low-frequency phase measurement with high-frequency squeezing," Opt. Express **20**, 18173–18179 (2012).
135. L. Zhang, K. Zheng, F. Liu, W. Zhao, L. Tang, H. Yonezawa, L. Zhang, Y. Zhang, and M. Xiao, "Quantum-limited fiber-optic phase tracking beyond π range," Opt. Express **27**, 2327–2334 (2019).
136. F. Mondain, T. Lunghi, A. Zavatta, É. Gouzien, F. Doutre, M. De Micheli, S. Tanzilli, and V. D'Auria, "Chip-based squeezing at a telecom wavelength," arXiv:1811.02097 (2018).
137. F. Kaiser, B. Fedrici, A. Zavatta, V. D'Auria, and S. Tanzilli, "A fully guided-wave squeezing experiment for fiber quantum networks," Optica **3**, 362–365 (2016).
138. H. Vahlbruch, D. Wilken, M. Mehmet, and B. Willke, "Laser power stabilization beyond the shot noise limit using squeezed light," Phys. Rev. Lett. **121**, 173601 (2018).
139. S. W. Lloyd, S. H. Fan, and M. J. F. Digonnet, "Experimental observation of low noise and low drift in a laser-driven fiber optic gyroscope," J. Lightwave Technol. **31**, 2079–2085 (2013).
140. Y. Cai, J. Roslund, G. Ferrini, F. Arzani, X. Xu, C. Fabre, and N. Treps, "Multimode entanglement in reconfigurable graph states using optical frequency combs," Nat. Commun. **8**, 15645 (2017).
141. N. P. Mauranyapin, L. S. Madsen, M. A. Taylor, M. Waleed, and W. P. Bowen, "Evanescent single-molecule biosensing with quantum-limited precision," Nat. Photonics **11**, 477–481 (2017).